Spectroscopic gas detection using a Bragg grating - stabilized external cavity laser, custom written in planar integrated silica-on-silicon

N. M. DAVIS,[1] S. G. LYNCH,[2] J. C. GATES,[2] J. HODGKINSON,[1,*] P. G. R. SMITH,[2] AND R. P. TATAM[1]

[1]*Engineering Photonics, Cranfield University, Cranfield, Bedfordshire, MK43 0AL, UK*
[2]*Optoelectronics Research Centre, University of Southampton, Southampton, Hampshire, SO17 1BJ, UK*
*j.hodgkinson@cranfield.ac.uk

Abstract: We present the development of an external cavity Bragg grating stabilized laser for tunable diode laser spectroscopy (TDLS). Our design uses a planar integrated silica-on-silicon platform incorporating a custom written Bragg grating as the wavelength-selective element of the laser cavity. We have developed a prototype singlemode laser at 1651 nm and performed a detailed characterization of its performance for the purpose of spectroscopic measurement of methane at this wavelength using a 25 cm path-length single-pass cell. Mode hop-free tuning of 0.13 nm has been demonstrated at frequencies of up to 10 kHz. A single-point limit of detection for TDLS of $\Delta I/I_0 = 8.3 \times 10^{-5}$ AU was achieved, which is consistent with the performance of standard distributed feedback lasers. The new device exhibits a side-mode suppression ratio of -40 dB and a low RIN of < -150 dB/Hz, and thus avoids the high levels of noise or instability normally associated with larger, mechanically driven external cavity lasers. The silica-on-silicon platform has the potential for low-volume manufacturing of special lasers at the custom wavelengths required for gas detection, without the need for investment in foundry solutions.

1. Introduction

Tunable diode laser spectroscopy (TDLS) is an important technique for the detection and quantification of trace atmospheric gases [1]. The emission wavelength of a laser is scanned across one or more gas absorption lines, usually in the near- or mid- infrared region, at a high resolution and the depth of the absorption line is related to the concentration of the target gas. The technique provides fast response times, high specificity to gas species and low limits of detection (LOD) [1]. Through a combination of low noise lasers and long optical pathlengths, gas concentrations can be resolved to levels in the parts per million (ppm) to parts per trillion (ppt) range.

Developments in optical telecommunications have resulted in semiconductor laser diodes with high reliability and residual intensity noise (RIN) of typically -140 dB/Hz or lower [2]. However, for gas lines outside the 1.3 μm or 1.55 μm telecoms bands, lasers must be fabricated at a particular wavelength, namely at the specific absorption line of the target gas. Laser diodes are often the technology of choice for many industrial and environmental applications, which require technological robustness and may be cost-sensitive. Significant investment is required to develop and manufacture the precise wavelengths required for specific gases, and yields may be limited by achievable manufacturing tolerances. The result is that the cost of a single laser can depend on the size of the market for detection of each gas species, or that specific wavelengths are not available in this format. This presents a problem for the detection of unusual gases in specialist applications, or for research that requires only limited quantities.

The mainstay of many gas detection instruments has been the distributed feedback (DFB) laser. This provides a stable and singlemode operating wavelength using a grating structure for optical feedback, usually written beyond the active wavelength region. Mode-hop free tuning is achieved either by changing the temperature of the device using a thermo-electric cooler (TEC) or by altering the injection current.

Vertical cavity surface emitting lasers (VCSELs) have emission perpendicular to the surface. This enables testing at numerous stages along the production process and enables the distribution of wavelengths across a wafer to be mapped. This helps to lower fabrication costs and has resulted in market penetration of VCSELs into price-sensitive applications. However, suppliers must still invest in a full wafer in order to produce a single device at any given wavelength. MEMS based VCSELs are under development; by adding a MEMS-actuated mirror to the top of the VCSEL, the tuning range is increased to 20 nm [3]. Manufacturing tolerances may be widened, thereby improving yields, and the ability to detect multiple gas species potentially increases the market.

Several attempts have been made to develop alternatives. Multimode absorption spectroscopy ("MUMAS") uses simpler, low cost multimode devices for gas detection. These have been realized using low cost, Fabry Perot devices [4] and in pumped Er:Yb:glass [5]. Finally, work is in progress to develop Bragg grating stabilized lasers, whereby the wavelength-selective element consists of an optical fiber Bragg grating (FBG) [6–8].

External cavity diode lasers (ECDLs) offer narrow linewidth operation and single-mode output with the ability to tune over a wide wavelength range [3]. The gain medium is a broadband gain chip, which is commercially available especially in the near IR region. The external cavity then typically incorporates a reflective grating as a wavelength-selective element, in the Littrow [9] or Littman–Metcalf [10] configurations. The gratings are typically rotated mechanically and / or driven using PZTs, which reduces robustness and stability, and adds to the laser's size and weight.

A further approach has been to include Bragg gratings integrated onto the laser chip, in distributed Bragg Reflector (DBR) structures. Using sampled gratings can extend the tuning range compared to standard DFB lasers and allows the gratings to be tuned independently of the gain medium. Tuning is rapid and mode hops are avoided using a phase control region. The devices have successfully been used for gas sensing of multiple gases owing to their wide tuning range [11]. However, such monolithic integration requires a foundry solution whereby small runs of devices at custom wavelengths would be difficult to justify.

The ECDL used in this work uses a planar silica-on-silicon platform incorporating a Bragg grating as both the wavelength selective element of the cavity and the feedback mirror. The integrated planar format allows direct writing of the waveguide and the Bragg grating itself, so that custom wavelengths may be written on demand with relatively low capital investment. Compared to conventional ECDLs, further advantages include robustness, desirable polarization properties and low noise. Planar gratings have been previously employed, for example, commercial devices offer high stability operation using Bragg grating stabilization [12]. We have reported a similar device in a planar waveguide using a related UV written Bragg grating [8,13], however to date such devices have not been demonstrated experimentally for gas sensing. In this paper, we report for the first time the use of a tunable laser based on planar silica-on-silicon in gas detection, a demanding application requiring high wavelength precision, mode-hop free tuning and low noise. Key research questions are, whether the precise wavelength required by gas sensing can be realized on demand, and whether the performance of the resulting laser is suitable for the application, specifically considering tuning performance and stability.

2.   Tunable diode laser spectroscopy of methane

Many gas molecules exhibit light absorption at specific wavelengths in the near and mid infrared regions of the electromagnetic spectrum. Tuning the emission from a singlemode laser across a single gas absorption line at high resolution enables quantification of the gas concentration via

the Beer-Lambert law [14]:

$$I = I_0 \exp(-\alpha L),$$

where I is the light transmitted through the gas cell, I_0 is the light incident on the gas cell, α is the absorption coefficient of the target gas species (typically with units cm^{-1}) and L is the cell's optical pathlength (typically with units of cm). The value of α is equal to ϵc, where ϵ is the specific absorptivity of the gas (units cm^{-1} atm^{-1}) and c is the gas concentration (typically in units of partial pressure, atm). For low αL this equation becomes linear and can be expressed as:

$$\frac{\Delta I}{I_0} \approx \alpha L,$$

where $\Delta I = I_0 - I$ and $\Delta I / I_0$ is defined as the absorbance, which is unitless but often expressed in terms of absorbance units (AU). The limit of detection of a target gas species can be quantified as the noise equivalent absorbance (NEA, in units AU) or the minimum detectable absorption coefficient (α_{min} in cm^{-1}), allowing instrumental techniques to be compared without reference to the specific target gas. For high resolution measurements of single gas lines made using a tunable laser, the value of I_0 is typically determined from a baseline measurement on either side of the absorption feature.

We consider the main application for our new technology to be the provision of lasers at specialist wavelengths that are unavailable or are uneconomic to produce in small quantities. Despite this, in this study we chose to work with methane (for which there is a well-established supply of DFB and VCSEL lasers) for several reasons. First, the principles of TDLS may be applied to different gas species via a change of wavelength and/or optical pathlength. Performance in terms of the NEA or α_{min} can often be translated from one species to another, within broadly the same wavelength regime. Second, there is considerable interest in detection and measurement of atmospheric methane for both industrial safety applications and environmental science. This means that there is considerable literature on the performance of TDLS based methane detectors that can be used for benchmarking purposes.

Figure 1 shows the absorption spectrum for methane in the 1650nm wavelength region, with an individual absorption line at 1651 nm highlighted. At atmospheric pressure, the linewidth (FWHM) is approximately 0.04 nm. To make a reliable, self-referenced measurement, the baseline at zero absorbance (as I_0) ideally needs to be measured on either side of the line, requiring a full scan of around 1nm. In order to reduce the effects of mechanical vibration on
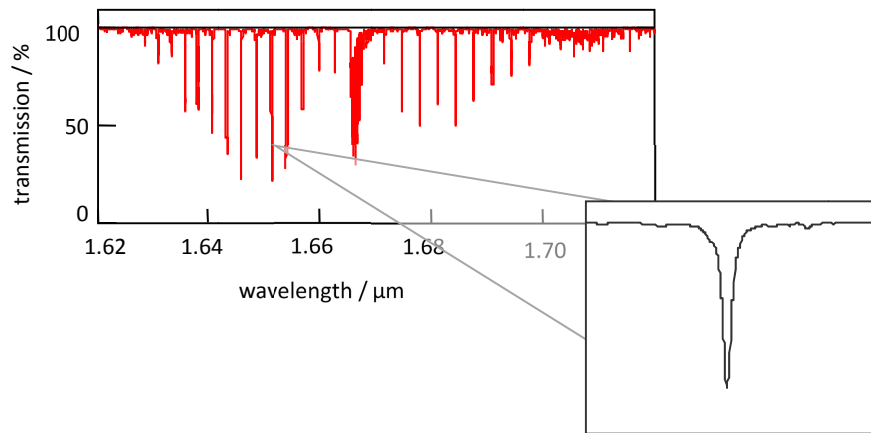

Fig. 1. Absorption spectrum for methane at 1650 nm, with an individual absorption line at 1651 nm highlighted.

laser alignment and to avoid 1/f noise in the electronics, scan frequencies in the kHz regime are preferred.

3.   External cavity Bragg stabilized laser

The external cavity Bragg stabilized laser (ECBSL) is formed from a semiconductor gain chip and a silica planar waveguide containing a Bragg grating. Figure 2 shows the internal layout of the laser assembly. The planar substrate of the Bragg grating chip was fabricated via flame-hydrolysis-deposition (FHD) and contains three layers of glass. The process started with a 1 mm thick silicon wafer, on which a 15 µm layer of oxide was thermally grown, this forms the underclad of the waveguide. Upon this a ~3.5 µm layer of silica glass was deposited via FHD and forms the photosensitive core layer. The photosensitivity was enabled by germanium doping and further enhanced by the addition of boron. A final layer of silica, again deposited by FHD, provides the overclad. This layer was ~7 µm thick and doped with phosphorus and boron, and as such was not UV photosensitive. The refractive index and thickness of the planar layers were chosen to aid coupling to the gain chip.
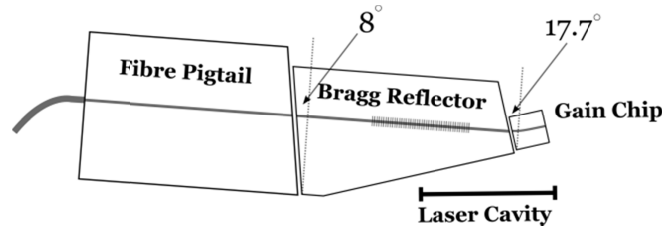

Fig. 2. Layout of external cavity Bragg grating stabilized laser, showing angled coupling to prevent parasitic reflections and optical fiber coupling.

The channel waveguide and Bragg grating were UV written by a single step process using 244 nm laser light, which increases the refractive index of the photosensitive core layer. Here two UV beams are focused into the photosensitive layer and the resulting interference forms a fringe pattern. The period and strength of this fringe pattern was controlled using an electro-optic modulator in one beam path. A complete description of this UV writing technique has been previously reported [15]. After writing, the planar waveguide chip was diced into a geometry to accommodate the heat sink supporting the gain chip and also to reduce parasitic back-reflections forming unwanted cavities. Near-optical quality finish of the diced surfaces was achieved using a physical machining technique [16]. Finally, a commercial v-groove assembly was butt coupled to the waveguide chip and secured using a UV adhesive layer to provide optical fiber coupling.

The small size writing spot used in the fabrication means that the grating design is software-controlled; specifically the central wavelength can be tuned over hundreds of nanometers. Gross changes to the center wavelength of the Bragg gating could be made by altering the angle at which the UV writing beams combined to form interference fringes. Together, these two controls enable the laser wavelength to be written on demand at minimal additional capital investment.

The ECBSL used a 1650 nm InP gain chip (Thorlabs SAF1091H). The gain chip had a highly reflective rear facet (90%) and an anti-reflective coated, angle terminated waveguide. To use the laser, the waveguide chip was butt coupled to the gain chip using a high precision, 3-axis positioning stage while observed using an optical microscope, as seen in Fig. 3(a). An image of the full laser assembly is shown in seen in Fig. 3(b). It is anticipated that a permanently packaged solution will be feasible in future work.
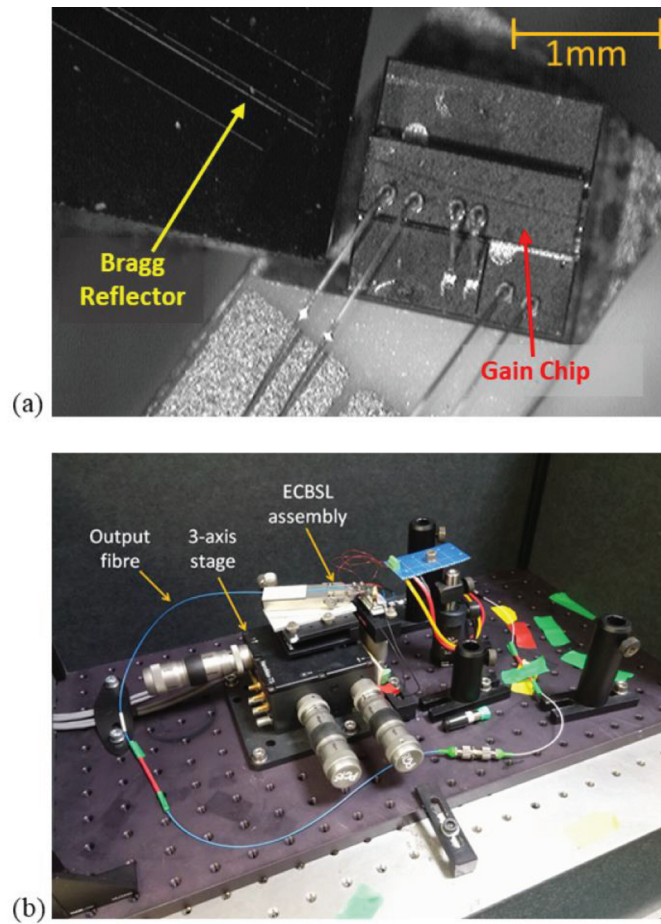
Fig. 3. External cavity Bragg stabilized laser. (a) Microscope image of alignment of Bragg reflector to gain chip (in the aligned state, the gap was reduced to ~ 20μm). (b) Experimental arrangement with microscope removed for clarity.

4. Experimental Results

4.1. External cavity Bragg stabilized laser performance

An example of the laser output spectrum can be seen in Fig. 4. The figure demonstrates that the device exhibits sidemode suppression ratios of >40 dB. It has also been noted that it has a relative intensity noise of <−150 dB/Hz [17] [1]. These figures are comparable to other commercially available ECDLs, with a pigtailed ECDL from Thorlabs (SFL1550S) demonstrating a relative intensity noise of −150 dB/Hz [18].

The temperature and current of the ECBSL's gain chip were controlled by a laser diode controller (Stanford Research Systems model LDC502). It was found that in this configuration, below current levels of 310 mA and above 410 mA the output of the laser would mode-hop, producing a sudden shift in wavelength, as seen in Fig. 5. It was therefore necessary to operate the laser within this current range to ensure mode-hop-free tuning.

To determine how the wavelength of the laser changed with injection current, the current was increased in steps of 5 mA between 310 mA and 410 mA with the wavelength output recorded.

Measurements of the laser output were taken using an OSA (with accuracy ± 0.1 nm and resolution 0.02 nm). The results are shown in Fig. 5.
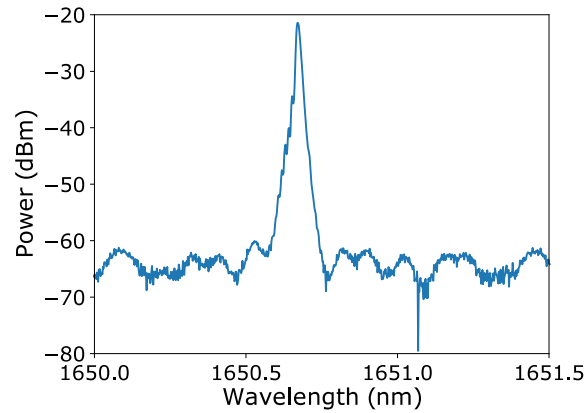

Fig. 4. Example of the output produced by the ECBSL. Data collected using an optical spectrum analyzer (Yokogawa AQ6370C).
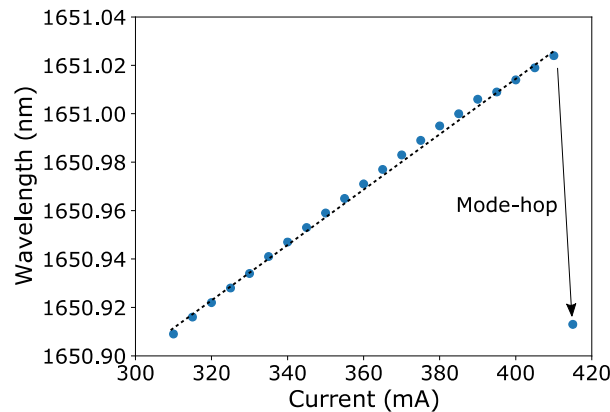

Fig. 5. Tuning Characteristics of the ECBSL. Points represent measured data, with the dashed line representing a linear trend line. An example of a mode-hop can be seen at 415 mA.

This tuning curve shows that the wavelength output of the laser increased by approximately 0.13 nm when the injection current is changed between the lower and upper current limits, providing a tuning coefficient of 1.3×10^{-3} nm/mA. Although this wavelength range is relatively small, it is sufficient to take measurements of the 1651 nm methane absorption line. Ideally a wider tuning range would permit better measurement of the absorption feature's baseline, but this is not essential. Mode hop-free tuning of the ECBSL was observed at modulation frequencies of up to 10 kHz, however, the tuning range at this frequency was slightly reduced, essentially limiting the current modulation to lower frequencies. A modulation frequency of 80 Hz was therefore used in further experiments.

4.2.   Methane Detection

A line diagram of the experimental set-up used to detect methane using the ECBSL can be seen in Fig. 6. To ensure that the tuning range of the laser was as large as possible, the laser emission

was modulated with a sawtooth waveform at 80 Hz using the output from a data acquisition module (Picoscope 5444B). This was then directed through a 25 cm single-pass gas cell with Brewster aligned windows. The beam was detected using a Thorlabs PDA400 amplified InGaAs detector, and the amplified signal collected using the data acquisition module and PC.
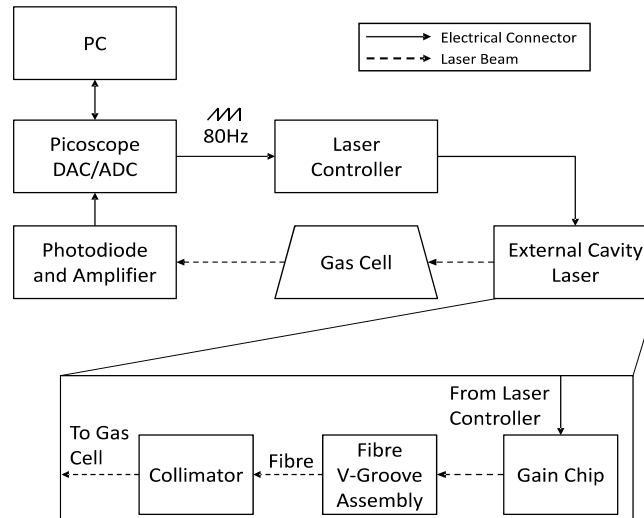

Fig. 6. Line diagram showing the set-up used to evaluate the ECBSL's suitability to detect methane.

To control the flow of methane and air being fed into the gas cell, methane and synthetic (hydrocarbon free) air cylinders were connected to a pair of mass flow controllers (Brooks Instrument model GF040CXX) regulated by a set point controller (Brooks Instrument 0254). Initially, a 2.5% methane in air cylinder was utilized to easily determine the correct current and temperature settings for the laser to align the absorption line with the center of the waveform. Measurements at lower concentrations were made using a cylinder containing 1010 ppm (∼0.1%) methane in air.

Figure 7 shows a comparison between the raw data collected for a measurement of synthetic air and of a measurement of 2.5% methane in air. The graph shows the limitations of the tuning range of the laser, with the width of the absorption line only just covered by the laser modulation. Due to the absorption line being slightly off-center in this measurement, the 2.5% methane reading does not quite meet the baseline at the bottom of the curve. This can then be seen clearly in Fig. 8, which displays the calculated absorbance from the measurement shown in Fig. 7. The laser wavelength during the scan (the x-axis in Fig. 8) was established by comparing the methane absorption line to data from the HITRAN database [19] for the same absorption feature.

By changing the flow rates from the cylinders, the concentration of methane in the gas cell could be adjusted. Using this technique, a range of concentrations were measured between 0 and 25,000 ppm (2.5% vol). Measurements were averaged over a 1 second period and then absorbance values for each measurement were calculated. In each case we simply recorded the peak absorbance value; the results can be seen in Fig. 9. The graph shows that the absorbance has a linear relationship with the concentration of methane in the cell.

It was found that the use of translation stages limited alignment stability of the laser to the optical fiber pigtail over time, which we attribute to thermal expansion and contraction of the stage components and supporting mounts. This cause noticeable changes to baseline readings when attempting to perform measurements below concentrations of around 100 ppm. This baseline drift prevented a clean measurement being made, restricting the concentration range that could
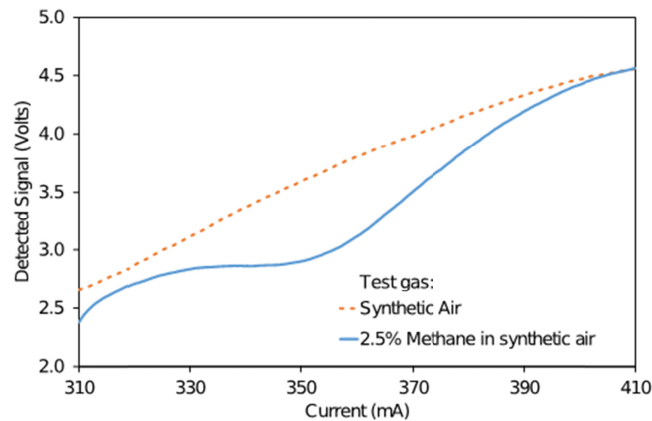
Fig. 7. Photodiode signal measured while the gain chip drive current was ramped in the range 310-410 mA. A rising output intensity indicates increased emission overall (test gas – synthetic air), while a methane absorption line can be observed in the output when methane was present.
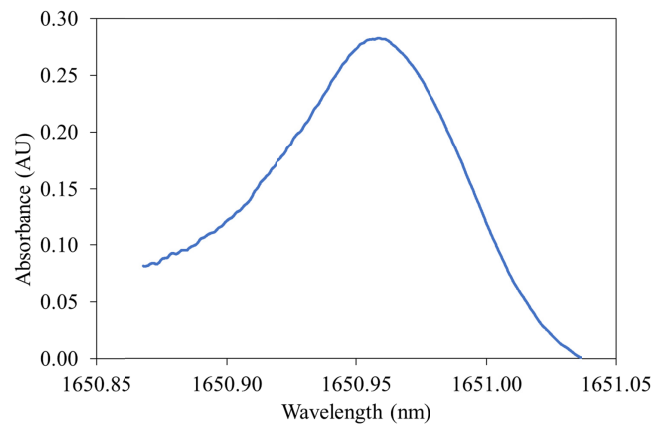

Fig. 8. Example of the calculated absorbance for 2.5% methane concentration detected using the ECBSL.

be analyzed. The effect of this can also be seen in Fig. 9 with relatively large error bars on data points around the linear fit. This scatter is likely attributable to fluctuations in the baseline as the error in the flow rate of the mass flow controllers is much smaller.

To determine the limit of detection, a calculation of the noise equivalent absorbance (NEA, in AU) using this set-up was performed using repeated synthetic air measurements and analyzing the RMS noise on the baseline. A standard deviation of 8.3×10^{-5} AU was estimated, and from this, a limit of detection could be calculated by comparing it to the peak absorbance at 100 ppm, resulting in a single-point LOD of 8.3 ppm. This is comparable to measurements made using a conventional DFB fiber-coupled laser, where a similar 8 ppm LOD was determined for a 25 cm pathlength single-pass gas cell using the same beam alignment [20]. It is therefore considered likely that, with fixed alignment of the laser to the output fiber, any noise or instability of the new laser would be reduced and it would be feasible to achieve measurements approaching the calculated limit of detection. Alternative sources of uncertainty include interference fringes from the gas cell, noise associated with the current driver and digitization within the detection system.
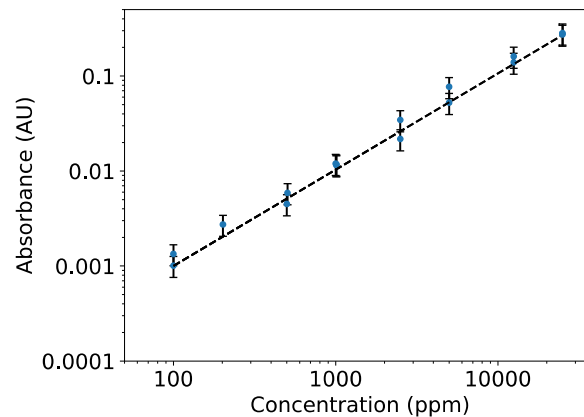
Fig. 9. Graph showing methane concentrations detected using the ECBSL versus their respective absorbance strengths. Large error bars are considered to be a consequence of the use of translation stages for alignment of the laser to the output fiber.

5. Discussion and conclusions

Investigations were performed into the suitability of utilizing a new external cavity Bragg-stabilized laser for use in methane detection. The laser tuning curve produced showed that the current tuning range of the ECBSL was just sufficient to cover the targeted methane absorption line. However, wider tuning would have enabled better determination of the measurement baseline.

It was found that the translation stages and mounts used to align the laser to the output fiber pigtail had limited stability, which affected baseline readings and introduced drift when making measurements below the level of approximately 100 ppm methane. The lack of stability of the laser also restricted the number of measurements that could be made at a time, as the gain chip and Bragg grating had to be realigned periodically. It is anticipated that this could be improved in future with laser packaging including permanent fixing of the fiber tip to the laser chip.

When the alignment was stable, repeated measurements of the baseline indicated that the single-point limit of detection (1σ) was 8.3×10^{-5} AU or 8.3 ppm, which was at a similar level to that of a conventional DFB laser. These results are encouraging and show the potential for improvement with better packaging.

We were able to modulate the laser at a frequency of 80 Hz, but at higher modulation frequencies (up to 10 kHz) the available wavelength modulation amplitude decreased. This would limit the use of techniques such as wavelength modulation spectroscopy (WMS), which under some circumstances can improve limits of detection. WMS requires large modulation amplitudes equal to $2.2 \times$ the gas linewidth [1], which for the methane absorption line at 1651 nm requires a peak-peak wavelength excursion of 0.088 nm (9.6 GHz) [21]. Although we exceeded this amplitude at low frequencies, for superior signal to noise ratios, operation is preferred at frequencies of approximately 1 kHz or higher. In future work we plan to address this limitation as follows. Thermal tuning of the Bragg grating can offer maximum tuning speeds of 31 GHz/ms at 1540 nm [22], which would correspond to 0.28 nm/ms at 1651 nm. WMS at this tuning speed could be obtained using a sinusoidal modulation frequency of approximately 1 kHz. An extended tuning range of up to 1.2 nm might also be feasible using an additional thermally tunable element of the waveguide to provide phase compensation during a scan and avoid mode hops [22]. The silica-on-silicon platform is considered capable of functioning with low loss at wavelengths up to around 2.2-2.3 μm.

To summarize, it has been shown that a new form of external cavity Bragg-stabilized laser can be used to detect methane in a laboratory set up, showing comparable NEA and LOD to a conventional DFB laser. The device has a much smaller form factor than a conventional external cavity laser, and no moving parts. The wavelength selective region has been decoupled from the gain region, potentially enabling commercially viable short runs of lasers with wavelength written "on demand". With improved packaging, the laser has the potential for gas detection performance similar to that of a conventional DFB laser diode.

Funding

Acknowledgments

References

1. J. Hodgkinson and R. P. Tatam, "Optical gas sensing: a review," Meas. Sci. Technol. **24**(1), 012004 (2013).
2. B. Lins, P. Zinn, R. Engelbrecht, and B. Schmauss, "Simulation-based comparison of noise effects in wavelength modulation spectroscopy and direct absorption TDLAS," Appl. Phys. B: Lasers Opt. **100**(2), 367–376 (2010).
3. S. Schilt, K. Zogal, B. Kögel, P. Meissner, M. Maute, R. Protasio, and M.-C. Amann, "Spectral and modulation preoperties of a largely tunable MEMS-VCSEL in view of gas phase spectroscopy applications," Appl. Phys. B: Lasers Opt. **100**(2), 321–329 (2010).
4. Y. Arita, R. Stevens, and P. Ewart, "Multi-mode absorption spectroscopy of oxygen for measurement of concentration, temperature and pressure," Appl. Phys. B: Lasers Opt. **90**(2), 205–211 (2008).
5. J. H. Northern, A. W. J. Thompson, M. L. Hamilton, and P. Ewart, "Multi-species detection using multi-mode absorption spectroscopy (MUMAS)," Appl. Phys. B: Lasers Opt. **111**(4), 627–635 (2013).
6. P. W. Juodawlkis, J. J. Plant, W. Loh, L. J. Missaggia, F. J. O'Donnell, D. C. Oakley, A. Napoleone, J. Klamkin, J. T. Gopinath, D. J. Ripin, S. Gee, P. J. Delfyett, and J. P. Donnelly, "High power, low-noise 1.5-μm slab-coupled optical waveguide (SCOW) emitters: physics, devices, and applications," IEEE J. Sel. Top. Quantum Electron. **17**(6), 1698–1714 (2011).
7. F. Chen, J. Hodgkinson, S. E. Staines, S. W. James, and R. P. Tatam, "A 1.65 μm region external cavity laser diode using an InP gain chip and a fibre Bragg grating," Proc. SPIE **8421**, 84215F (2012).
8. S. G. Lynch, F. Chen, J. C. Gates, C. Holmes, S. E. Staines, S. W. James, J. Hodgkinson, P. G. R. Smith, and R. P. Tatam, "Bragg-grating-stabilized external cavity lasers for gas sensing using tunable diode laser spectroscopy," Proc. SPIE **9002**, 900209 (2014).
9. L. Ricci, M. Weidemüller, T. Esslinger, A. Hemmerich, C. Zimmermann, V. Vuletic, W. König, and T. W. Hänsch, "A compact grating-stabilized diode laser system for atomic physics," Opt. Commun. **117**(5-6), 541–549 (1995).
10. M. G. Littman and H. J. Metcalf, "Spectrally narrow pulsed dye laser without beam expander," Appl. Opt. **17**(14), 2224–2227 (1978).
11. K. Boylan, V. Weldon, D. McDonald, J. O'Gorman, and J. Hegarty, "Sampled grating DBR laser as a spectroscopic source in multigas detection at 1.52-1.57 μm," IEE Proc.: Optoelectron. **148**(1), 19–24 (2001).
12. M. Alalusi, P. Brasil, S. Lee, P. Mols, L. Stolpner, A. Mehnert, and S. Li, "Low noise planar external cavity laser for interferometric fiber optic sensors," Proc. SPIE **7316**, 73160X (2009).
13. S. G. Lynch, C. Holmes, S. A. Berry, J. C. Gates, A. Jantzen, T. I. Ferreiro, and P. G. R. Smith, "External cavity diode laser based upon an FBG in an integrated optical fiber platform," Opt. Express **24**(8), 8391–8398 (2016).
14. J. D. Ingle and S. R. Crouch, *Spectrochemical Analysis* (Prentice Hall, 1988).
15. C. Sima, J. Gates, H. Rogers, P. Mennea, C. Holmes, M. Zervas, and P. Smith, "Ultra-wide detuning planar Bragg grating fabrication technique based on direct UV grating writing with electro-optic phase modulation," Opt. Express **21**(13), 15747–15754 (2013).
16. L. G. Carpenter, H. L. Rogers, P. A. Cooper, C. Holmes, J. C. Gates, and P. G. R. Smith, "Low optical-loss facet preparation for silica-on-silicon photonics using the ductile dicing regime," J. Phys. D: Appl. Phys. **46**(47), 475103 (2013).
17. S. G. Lynch, "Integrated planar cavities for external cavity diode lasers," PhD Thesis, University of Southampton, Southampton, UK (2017).
18. Thorlabs, Inc., "SFL1550S - 1550 nm, 40 mW, Butterfly External Cavity Laser, SM Fiber, FC/APC," [Online]. Available: https://www.thorlabs.de/thorproduct.cfm?partnumber=SFL1550S

19. I. E. Gordon, L. S. Rothman, C. Hill, R. V. Kochanov, Y. Tan, P. F. Bernath, M. Birk, V. Boudon, A. Campargue, K. V. Chance, B. J. Drouin, J.-M. Flaud, R. R. Gamache, J. T. Hodges, D. Jacquemart, V. I. Perevalov, A. Perrin, K. P. Shine, M.-A. H. Smith, J. Tennyson, G. C. Toon, H. Tran, V. G. Tyuterev, A. Barbe, A. G. Császár, V. M. Devi, T. Furtenbacher, J. J. Harrison, J.-M. Hartmann, A. Jolly, T. J. Johnson, T. Karman, I. Kleiner, A. A. Kyuberis, J. Loos, O. M. Lyulin, S. T. Massie, S. N. Mikhailenko, N. Moazzen-Ahmadi, H. S. P. Müller, O. V. Naumenko, A. V. Nikitin, O. L. Polyansky, M. Rey, M. Rotger, S. W. Sharpe, K. Sung, E. Starikova, S. A. Tashkun, J. Vander Auwera, G. Wagner, J. Wilzewski, P. Wcisło, S. Yu, and E. J. Zak, "The HITRAN2016 molecular spectroscopic database," J. Quant. Spectrosc. Radiat. Transfer **203**, 3–69 (2017).
20. N. M. Davis, "Mid-infrared spectroscopic instrumentation for airborne monitoring of atmospheric gas species," PhD Thesis, Cranfield University, Cranfield, UK (2018).
21. J. Hodgkinson, D. Masiyano, and R. P. Tatam, "Using integrating spheres with wavelength modulation spectroscopy: effect of pathlength distribution on 2nd harmonic signals," Appl. Phys. B: Lasers Opt. **110**(2), 223–231 (2013).
22. C. Holmes, D. O. Kundys, J. C. Gates, C. B. E. Gawith, and P. G. R. Smith, "150 GHz of thermo-optic tuning in direct UV written silica-on-silicon planar Bragg grating," Electron. Lett. **45**(18), 954–956 (2009).